Journal of Applied Research in Water and Wastewater
E-ISSN: 2476-6283
Journal homepage: https://arww.razi.ac.ir

Pathogen removal from simulated hospital wastewater via plant-mediated Ag nanoparticles synthesized with Ferula assa-foetida extract

Hassan Koohestani*, Ali Balooch

Faculty of Materials and Metallurgical Engineering, Semnan University, Semnan, Iran.

GRAPHICAL ABSTRACT

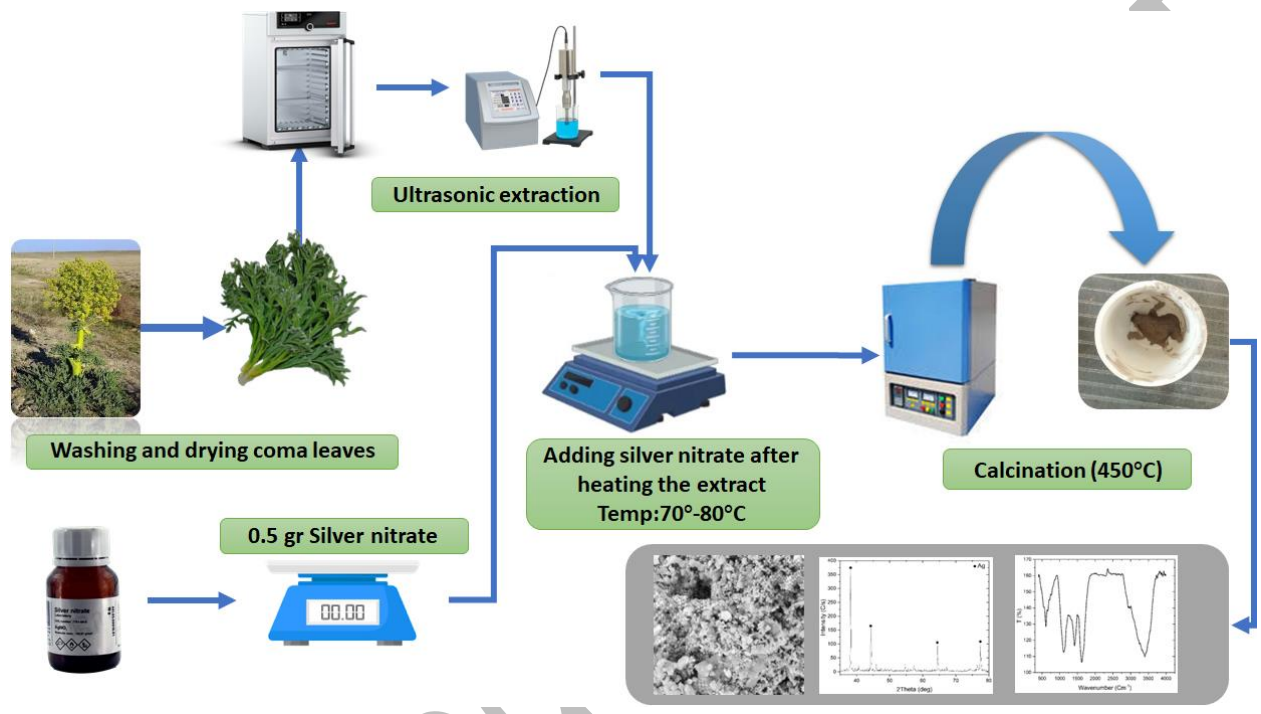

ARTICLE INFO

Article type:
Research Article

Article history:
Received xx Month xxx
Received in revised form xx Month xxx
Accepted xx Month xxx
Available online x Month xx

Keywords:
Wastewater
Ag nanoparticles
Biosynthesized
Antibacteria
Antiviral
Hospital

ABSTRACT

The present study outlines the production of AgNPs through a green synthesis method utilizing the water extract of Ferula assa-foetida leaves. In contrast to earlier studies that mainly focused on the plant's gum, this research used an ultrasonic-assisted extraction method for the leaf tissues. FTIR analysis validated the presence of different organic compounds, particularly phenolic groups, on the AgNPs surface, which is crucial for their stability and bioactivity. FE-SEM images displayed the nanoparticles' shapes, which were mainly spherical and cauliflower-like, with an average size of 86 nm. XRD analysis revealed that silver ions were reduced to create metallic nanoparticles in the following phase, as shown by distinctive peaks at 38.2°, 44.4°, and 64.51°. Synthesized nanoparticles were assessed for antibacterial properties against two bacterial models: Staphylococcus aureus (Gram-positive) and Escherichia coli (Gram-negative). A higher sensitivity was observed in Gram-positive bacteria. Therefore, AgNPs produced using Ferula leaf extract can be considered valuable alternatives for antibacterial and therapeutic purposes.

1. Introduction

Water, being an essential resource, is crucial for the survival of living organisms; nevertheless, the deterioration of water quality due to human actions has presented considerable risks to environmental well-being (Naeini, 2025). As the population grows and industrial activities intensify, water pollution is on the rise. A significant contributor to this pollution is the discharge from numerous industries, including those in the chemical and metal sectors, as well as wastewater from hospitals, which is laden with high concentrations of microbes and chemical

*Corresponding author Email: h.koohestani@semnan.ac.ir

Cite this article: H. Koohestani, A. Balooch, Pathogen removal from simulated hospital wastewater via plant-mediated Ag nanoparticles synthesized with Ferula assa-foetida extract, *Journal of Applied Research in Water and Wastewater*, x (x), 202x, xx-xx. doi: https://doi.org/10.22126/arww.2025.12392.1387

pollutants. Key factors that notably diminish the quality and usability of water resources include water hardness, the presence of heavy metals, and microbial contamination (Anyanwu *et al.*, 2024; Koohestani and Gohariyan Bajestani, 2025).

Pathogenic bacteria infect or cause the death of more than 15 million people worldwide each year and contaminate food and water resources. Among the most important are Escherichia coli (responsible for urinary tract infections), Staphylococcus aureus (responsible for food poisoning), Pseudomonas aeruginosa (a cause of hospital-acquired infections), Salmonella typhi (the cause of typhoid fever), and Shigella (a cause of severe diarrhea) (Salehi Reyhani and Khoshnood, 2020; Zadeh, Kashanian, and Nazari, 2024).

Eco-friendly or biogenic nanoparticle synthesis using plant-derived extracts has emerged as a cost-effective and sustainable alternative. This method relies on bioactive secondary metabolites, such as phenolic compounds, flavonoids, terpenes, and alkaloids, that serve dual roles in reduction and stabilization (Ahmed et al., 2016).

Extensive research has examined the antibacterial properties of silver nanoparticles (AgNPs). Their antimicrobial mechanism involves interaction with the microbial cell wall, altering its permeability and ultimately leading to cell death. In addition, AgNPs can generate reactive oxygen species (ROS) and interfere with enzymatic systems, leading to cellular damage. Beyond their antibacterial role, these nanoparticles have also been reported to suppress the growth of cancer cells (Hajipour *et al.*, 2012; Koohestani, Nabilo, and Balooch, 2024).

In eco-friendly synthesis approaches, different plant species have been utilized to act as both reducing and stabilizing agents in the formation of silver nanoparticles. Notable examples of these plants include Oscillatoria (Adebayo-Tayo, Salaam, and Ajibade, 2019), Azadirachta indica (Ahmed *et al.*, 2016), Ziziphora, Wild barberry, Melder, and Hawthorn (Koohestani, Nabilo, and Balooch, 2024). The utilization of such natural resources not only promotes the creation of nanoparticles with enhanced stability and controlled dimensions but also improves their biological efficacy due to the intrinsic medicinal properties of the plant extracts-especially in antibacterial and anticancer contexts (Koohestani, Nabilo, and Balooch, 2024; Taleb Safa and Koohestani, 2024).

Although the resin of Ferula assa-foetida has been applied in nanoparticle synthesis and antibacterial studies, reports on using its leaf extract are lacking. This research demonstrates the synthesis of silver nanoparticles from the leaves and examines their application in treating hospital wastewater.

A multitude of studies have shown various biological activities associated with extracts from plants belonging to the *Ferula*, which encompass anticancer, antimicrobial, anti-inflammatory, and anti-ulcer effects. These extensive properties validate the significant potential of these plants for use in pharmaceutical and therapeutic contexts (Mohammadhosseini et al., 2019; Sahebkar and Iranshahi, 2010).

This work focused on silver nanoparticles synthesized from Ferula leaf extract and explored their structural, physicochemical, and antibacterial attributes. The characterization included assessment of morphology, particle size, crystalline nature, surface functional groups, and thermal behavior. X-ray diffraction (XRD) was employed to confirm the crystalline structure, while dynamic light scattering (DLS) provided information regarding the size distribution and polydispersity index of the nanoparticles. Fourier-transform infrared spectroscopy (FTIR) was used to identify the functional groups involved in nanoparticle capping and stabilization. Morphological features and surface characteristics were examined through field emission scanning electron microscopy (FE-SEM), while simultaneous thermal analysis (STA) assessed thermal stability and the presence of residual organic compounds. The antibacterial activity of the AgNPs was thoroughly assessed against Gram-positive and Gram-negative bacteria, highlighting their potential use in antimicrobial applications, especially for treating hospital wastewater.

2. Materials and methods

This study used silver nitrate ($AgNO_3$, 99.5%, DRM CHEM company, Iran) and nitric acid (HNO_3, 65%, Merck, Germany).

2.1. Extract method

The leaves of *Ferula Assa-foetida* were initially gathered from the Eshqabad region in South Khorasan, Iran, and subsequently sun-dried for one week. The dried leaves were ground using a mortar and combined with distilled water (10 g in 50 mL). The resulting mixture was agitated in an ultrasonic bath for 15 min. Finally, the extraction was completed utilizing filter paper (Balooch *et al.*, 2025; Koohestani, Nabilo, and Balooch, 2024).

2.2. Synthesis of AgNPs

Silver nanoparticles (AgNPs) were prepared using $AgNO_3$ as the precursor, FLE as a reducing agent, and deionized water as the solvent. Initially, 35 mL of the extract was transferred into a covered vessel and heated on a hot plate at 75-80°C. Subsequently, 0.5 g of silver nitrate was added, and the mixture was stirred for 10 minutes. To aid the complete dissolution of silver nitrate, 5 µL of nitric acid (HNO_3) was gradually introduced at 5-second intervals. The resulting solution was then continuously stirred at 70-80°C for 2 hours. The final concentration of $AgNO_3$ was approximately 84 mM. After completion, the solution was left uncovered to allow water evaporation, and the resulting paste was calcined at 450 °C and 650 °C to obtain the final nanoparticles.

2.3. Characterization

The nanoparticles were characterized for their crystallinity using X-ray diffraction (XRD, Cu-Kα, λ = 0.1544 nm, 2θ = 10–90°; Bruker D8 Advance, Germany). Particle size and PDI were measured by dynamic light scattering (DLS, Nano-ZS90, Malvern, UK), while Fourier-transform infrared spectroscopy (FTIR, Shimadzu 8400S, Japan) investigated extract-nanoparticle interactions after powdering the extract at 110°C for 2 h. Field emission scanning electron microscopy (FE-SEM, Zeiss Sigma 300-HV, Germany) revealed morphology, and simultaneous thermal analysis (STA, LINSEIS PT-1000, Germany) evaluated thermal behavior and stability via simultaneous thermogravimetric analysis (TGA) and differential thermal analysis (DTA).

2.4. Assessment of antibacterial and antiviral

To replicate a hospital wastewater environment, an artificial medium was prepared containing peptone (5 g/L), yeast extract (3 g/L), glucose (1 g/L), urea (0.5 g/L), NaCl (8.5 g/L), and Triton X-100 (0.05%) as a nonionic detergent. The medium was buffered to pH 7.2 with phosphate solution and sterilized through autoclaving. Standard bacterial strains, E. coli (ATCC 25922, a Gram-negative bacterium) and S. aureus (ATCC 6538, a Gram-positive bacterium), were inoculated at ~10^6 CFU/mL to simulate typical hospital wastewater microbial loads.

The antibacterial effects of AgNPs synthesized *using Ferula assa-foetida* extract (*FAgNPs*) were investigated using multiple complementary techniques. For the colony-forming unit (CFU) assay, bacteria treated with 50 and 100 µg/mL of nanoparticles were spread onto nutrient agar plates and incubated at 37 °C for 24 hours. The resulting colonies were counted and compared to untreated controls. Additionally, bacterial growth was monitored more rapidly by measuring the optical density at 600 nm (OD600) with a spectrophotometer.

Additionally, the disk diffusion assay was performed on Mueller-Hinton agar plates; filter paper discs soaked with FAgNPs were placed on bacterial lawns, and the diameters of inhibition zones were measured. The minimum inhibitory concentration (MIC) was determined using the broth dilution method to identify the lowest nanoparticle concentration that visibly inhibited bacterial growth.

To assess the antiviral efficacy of the FAgNPs, human adenovirus type 5 (HAdV-5) was used as a model for a non-enveloped DNA virus. The evaluation of viral inhibition was conducted using real-time PCR, with a focus on the hexon gene. After treatment with the nanoparticles, viral DNA was extracted and subsequently amplified using designated primers (forward: 5'-GCCACGGTGGGGTTTCTAAACTT-3', reverse: 5'-GCCCCAGTGGTCTTACATGCACATC-3'). The reduction in viral load was measured by comparing Ct values to those of untreated controls, thereby indicating the inhibitory impact of FAgNPs on the replication of HAdV-5.

3. Results and discussion

The FE-SEM images (Figs. 1a and 1b) show that the *FAgNPs* have a predominantly spherical to ellipsoidal shape with a cauliflower-like surface texture and a moderate tendency to agglomerate, which is generally attributed to interparticle forces at the nanoscale.

According to the Digimizer-based size distribution analysis (Fig. 1c), the nanoparticles measured between 40 and 140 nm, and their average size was nearly 86 nm. This is smaller than the sizes reported in previous studies by Hashemi (200–500 nm) and Nasiri (120 nm). This reduced size may contribute to enhanced antibacterial activity due to the increased specific surface area. Furthermore, EDX analysis (Fig. 1d) confirmed a high silver content of over 67 wt% in the prepared nanostructure. Overall, the cauliflower-like morphology, nanoscale size distribution, and high silver purity render these *FAgNPs* highly promising for antibacterial and biomedical applications (Hashemi *et al.*, 2022; Nasiri *et al.*, 2018).

The thermal characteristics of the *FAgNPs* were examined through STA, which encompasses TGA and DTA. According to Fig. 2, a reduction of around 20 mg in mass is observed below 200 °C in the TGA plot, which is attributed to moisture desorption and the breakdown of extract-based organic stabilizing compounds. Beyond 200 °C, the weight remained relatively stable up to 800 °C, indicating the remarkable thermal stability of the metallic silver core following the elimination of organic materials.

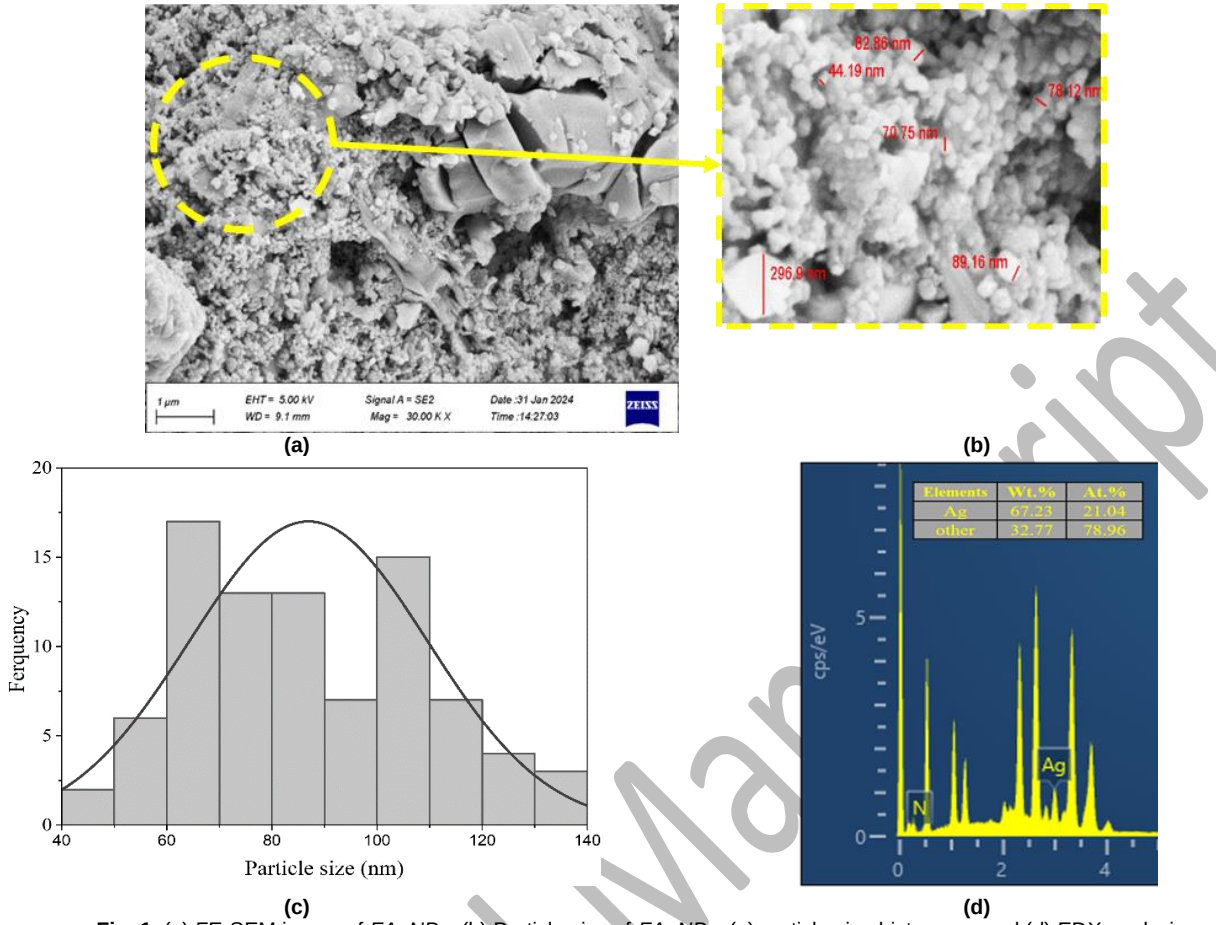

Fig. 1. (a) FE-SEM image of *FAgNPs*, (b) Particle size of *FAgNPs*, (c) particle size histogram, and (d) EDX analysis.

The DTA signal exhibited an endothermic peak within the range of 50–200 °C, corresponding to the evaporation of water, followed by a minor exothermic peak around 150-200 °C, likely associated with the combustion or oxidative degradation of the plant-derived capping agents. Above 200 °C, only slight variations were noted in the DTA signal, further affirming the thermal resilience and structural integrity of the *FAgNPs*. In summary, these results confirm that the green-synthesized silver nanoparticles exhibit high thermal stability and structural durability, thereby endorsing their applicability across various environmental conditions (Adebayo-Tayo, Salaam, and Ajibade, 2019; John *et al.*, 2021; Labulo, David, and Terna, 2022).

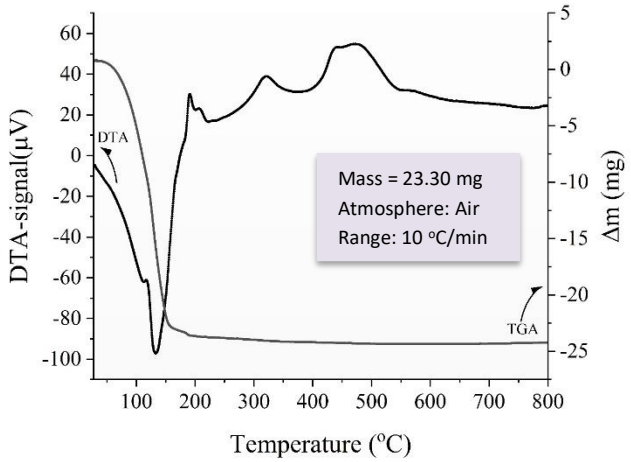

Fig. 2. Thermograph TGA and DTA *FAgNPs*

As shown in Fig. 3, the XRD profile of FAgNPs is marked by reflections positioned at 38.2°, 44.4°, and 64.51°. These peaks correspond to the (111), (200), and (220) crystallographic planes of silver and validate the presence of a face-centered cubic arrangement, in line with the JCPDS standard file 90-08459. The dominant signal at 38.2° suggests a preferred alignment along the (111) plane. Using the Scherrer equation, the average crystallite size of the nanoparticles was derived (Eq.1) (Koohestani, Nabilo, and Balooch, 2024):

$$D = \frac{k\lambda}{(\beta cos\theta)} \quad (1)$$

In the Scherrer relation, the crystallite dimension (D) can be estimated from the broadening of the diffraction peaks. This calculation considers the diffraction angle (θ), the peak width at half of its maximum height (β, expressed in radians), the wavelength of the X-ray source (λ, which is 1.54 Å for Cu Kα radiation), and a shape constant (K, generally assumed as 0.9). Using this approach, the average crystallite size of the *FAgNPs* was found to be 35.6 nm and 35.7 nm after calcination at 450 °C and 650 °C, respectively. Previous investigations, such as those involving extracts of wild barberry, medlar (Mespilus germanica L.), and hawthorn, reported XRD peaks positioned at 38.1°, 51.56°, 64.46°, and 77.42°, corresponding to the (111), (311), (200), and (220) reflections of silver (Koohestani, Nabilo, and Balooch, 2024). Comparable crystallite sizes, close to 34.5 nm, have also been documented for AgNPs synthesized using plant extracts such as green tea (Taleb Safa and Koohestani, 2024), Ferula asafoetida (Valinezhad, Talebi, and Alamdari, 2023), medlar, Nigella sativa (Adebayo-Tayo, Salaam, and Ajibade, 2019), and Ziziphora clinopodioides (Esmaile, Koohestani, and Abdollah-Pour, 2020).

In green synthesis, secondary metabolites such as terpenes, flavonoids, and alkaloids help reduce silver ions while simultaneously stabilizing the resulting nanoparticles, thereby offering an eco-friendly alternative to conventional chemicals. To verify the functional groups attached to the AgNPs, FTIR measurements were taken within the 400–4000 cm^{-1} spectral window. The resulting profile, illustrated in Fig. 4 and summarized in Table 1, exhibits several diagnostic peaks. Among them, the broad absorption near 3425 cm^{-1} is indicative of O–H stretching vibrations typical of hydroxyl-containing groups (Koohestani, Balooch, and Hasanpoor, 2024; Labulo, David, and Terna, 2022).

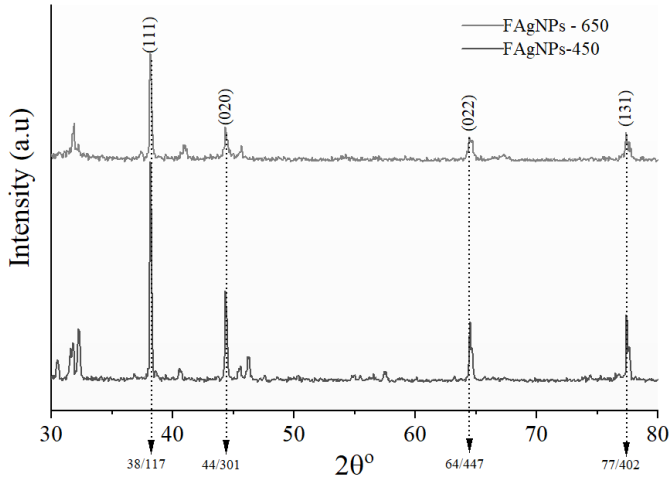

Fig. 3. XRD pattern of synthesized *FAgNPs* after calcination.

Based on Fig. 4, the absorption feature at 1436 cm^{-1} corresponds to the S=O stretching mode of sulfate groups (Nie *et al*., 2023), which confirms the presence of sulfur and is in line with earlier reports on this plant (Balooch *et al*., 2025). Additional signals at 1188 cm^{-1} and 1107 cm^{-1} arise from C-O stretching vibrations, typical of secondary alcohols (Seki *et al*., 2013). The broad band detected near 617 cm^{-1} is linked to Ag-Ag metal interactions (Augustine *et al*., 2020; Smuleac *et al*., 2011). Interestingly, after silver reduction, the original absorption at 605.61 cm^{-1} shifted to 617.18 cm^{-1} (Valinezhad, Talebi, and Alamdari, 2023), suggesting alterations in bonding characteristics upon nanoparticle formation.

A generalized equation representing the reduction of silver can be expressed as illustrated in Fig. 4 (Koohestani, Nabilo, and Balooch, 2024; Smuleac *et al*., 2011).

$$C_6H_6OH + 2AgNO_3 \rightarrow C_6H_4O_2 + 2Ag + 2HNO_3 \quad (2)$$

The proposed mechanism suggests that *phenol* groups facilitate the reduction of *FAgNPs*. FTIR analyses have demonstrated that during this reduction process, a significant conversion of *hydroxyl* groups to *carbonyls* occurs. Furthermore, *AgNPs* synthesized from green plant extracts may exhibit synergistic effects, leveraging the combined properties of both the plant extract and the nanoparticles. Numerous studies have highlighted that the characteristics of *AgNPs* are influenced by the specific plant extract utilized in their synthesis, underscoring the importance of the plant's nature in this context (Adebayo-Tayo, Salaam, and Ajibade, 2019). Additionally, phenolic and polyphenolic compounds, whether used individually or in conjunction with vitamins such as carotenoids, vitamin E, and vitamin C, function as antioxidants, safeguarding human tissues against the detrimental impacts of oxidative stress. Polyphenols are prevalent antioxidants found in diets rich in fruits and vegetables, playing a key role in the prevention of chronic diseases.

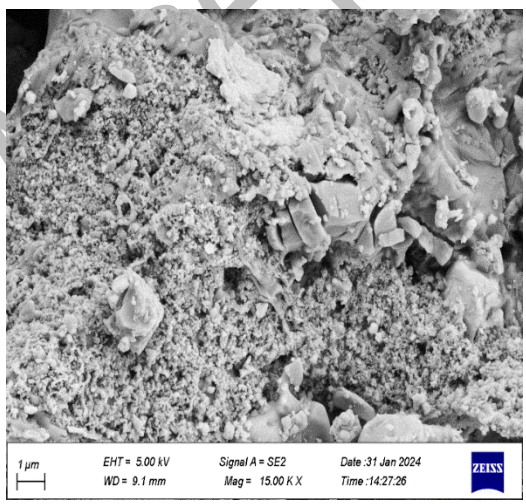

(a)

Table 1. Functional groups identified by FTIR spectroscopy of *FAgNPs* and *FLE*.

Wavenumber(cm^{-1})		Bond type	Functional groups
AgNPs	617.18	Ag-Ag	metallic bond
	999.06	N-H	alkyl halides, amines
	1188.07	C-O	Stretching, type II alcohol
	1436.87	S=O	Sulfate ester
	3425.34	O–H	hydroxyl group, phenol groups
FLE	605.61	M-O	metallic bond
	1110.92	C-H, C-O	flavonoid groups, aliphatic amine
	1415.65	S=O	Sulfate ester
	1620.09	C=C	vibrations of the aromatic bond
	3404.13	O-H	hydroxyl group, phenol groups

DLS was utilized to assess the hydrodynamic size distribution and zeta potential of *FAgNPs*. As illustrated in Fig. 5 (b), the distribution of particle sizes varied from approximately 10 to 180 nm, with a predominant population observed between 20 and 60 nm, indicating a relatively narrow and uniform dispersion profile. This slight increase in size compared to the results obtained from FE-SEM may be attributed to the organic capping agents originating from the plant extract, which form a hydration shell around the nanoparticles in the colloidal suspension.

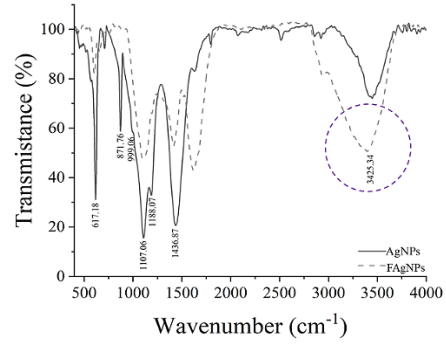

(a)

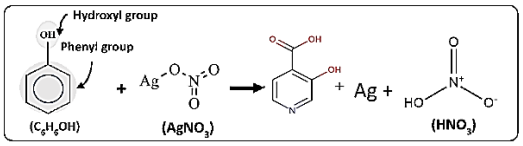

(b)

Fig. 4. (a) FTIR spectra of *FAgNPs* and the plant extract (*FLE*), and (b) the reduction reaction between silver nitrate and the functional groups present in the *FLE*.

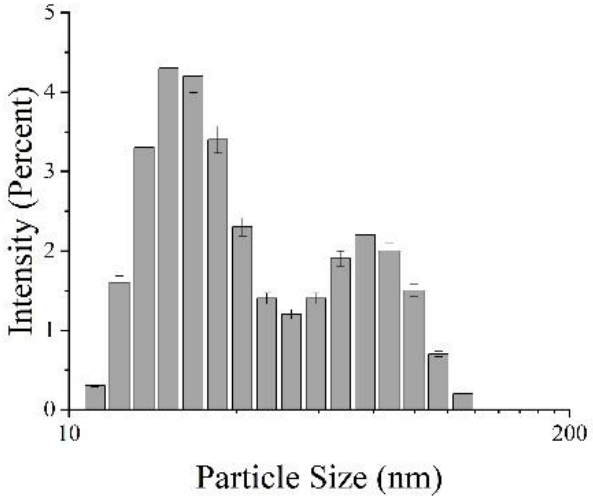

(b)

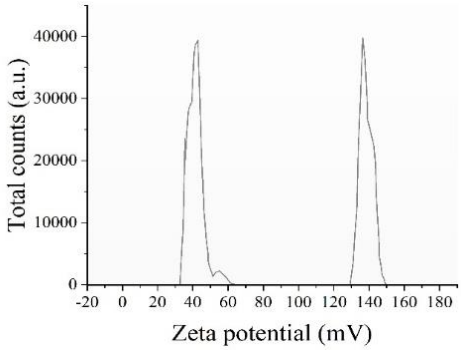

(c)

Fig. 5. (a) FE-SEM image, (b) particle size distribution, and (c) zeta potential distribution of *FAgNPs*.

Furthermore, the zeta potential analysis (Fig. 5(c)) displayed two significant peaks at approximately 40 mV and 125 mV, indicating the existence of particle populations with distinct surface charge characteristics, thus supporting the high electrostatic stability of the colloidal system. The variety of phytochemicals found in plant extracts, such as *terpenes*, *flavonoids*, and *alkaloids*, plays a crucial role in the variations observed in particle size and surface charge. Similar studies have reported analogous findings; for instance, Adebayo-Tayo *et al.* (Adebayo-Tayo, Salaam, and Ajibade, 2019) documented AgNPs with a size of 558.1 nm and a Polydispersity Index (PDI) of 0.580, while Subramaniam *et al.* (Subramaniam et al., 2022) synthesized AgNPs from Ferula assa-foetida with an average size of 100 nm, a low PDI of 0.3, and a zeta potential of –36.7 mV. Collectively, these findings validate that the green synthesis approach utilizing *FLE* facilitates the production of stable, well-dispersed silver nanoparticles suitable for biomedical applications. The electrostatic properties of bacterial surfaces arise from the molecular composition of the cell wall, with groups such as phosphates, amines, and carboxyls contributing to the overall charge distribution. Gram-positive bacteria commonly show a net positive surface charge, which is attributed to their dense peptidoglycan layer. Conversely, Gram-negative species are usually negatively charged because of lipopolysaccharide structures within the outer membrane (Joshi, Singh, and Mijakovic, 2020; Koohestani, Nabilo, and Balooch, 2024). Metallic nanoparticles, unlike bacteria, have frequently been described as carrying negative surface charges, a feature relevant to their interactions with microbial cells (Slavin *et al.*, 2017).

Nonetheless, various mechanisms might play a role in the biological functions, including antiviral and antibacterial properties, particularly when silver nanoparticles are produced through environmentally friendly methods utilizing plant extracts. These biogenic nanoparticles can directly attach to the surfaces of bacterial or eukaryotic cells, compromising their structural integrity. Once they penetrate the cytoplasm, they can engage with organelles and cellular macromolecules, produce reactive oxygen species (ROS), inflict damage on membranes, and ultimately interfere with electron transport processes (Abootalebi *et al.*, 2021; Kędziora *et al.*, 2018; Mikhailova, 2020; Rasheed *et al.*, 2023; Roy *et al.*, 2019). As shown in Fig. 6, FAgNPs demonstrated significant antibacterial activity against both Gram-negative (Escherichia coli) and Gram-positive (Staphylococcus aureus) bacteria. According to CFU assessments, a treatment involving 100 µg/mL of AgNPs led to a reduction exceeding 90% in bacterial populations for both bacterial strains. For instance, the CFU count for E. coli diminished from 1.0×10^6 to 0.8×10^5, signifying potent bactericidal effects even against more resistant strains. The OD600 measurements revealed that bacterial growth was markedly reduced following AgNP treatment. While the control cultures exhibited normal exponential growth for approximately 12 hours, the treated samples stabilized at an optical density of about 0.43, reflecting growth suppression by the nanoparticles. In the disk diffusion test, inhibition zones measured 14 mm for E. coli and 16 mm for S. aureus at 100 µg/mL of AgNPs. Although gentamicin generated slightly larger clear zones, the silver nanoparticles displayed a comparable antibacterial effect. The MIC analysis further indicated values of 25 µg/mL for S. aureus and 37.5 µg/mL for E. coli, highlighting the greater vulnerability of Gram-positive bacteria to AgNP exposure.

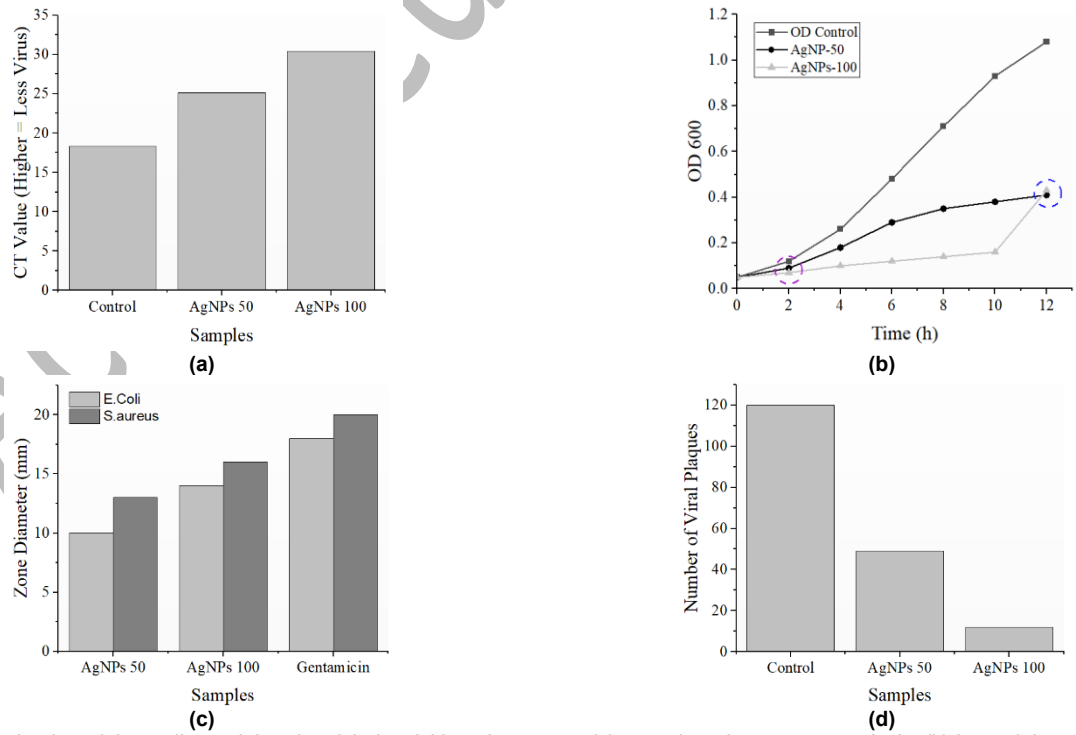

Fig. 6. Evaluation of the antibacterial and antiviral activities of *FAgNPs*: (a) CT values from qPCR analysis, (b) bacterial growth curves (OD600), (c) inhibition zone diameters against E. coli and S. aureus compared to gentamicin, and (d) number of viral plaques.

The antiviral capabilities of the *FAgNPs* were assessed through real-time polymerase chain reaction (qPCR) and plaque assays. The Ct value for the viral gene in the untreated control group was recorded at 18.3, indicating a high level of viral replication. Following treatment with *FAgNPs* at concentrations of 50 and 100 µg/mL, the Ct values rose to 25.1 and 30.4, respectively, reflecting a robust suppression of viral gene

expression. Likewise, the plaque assay revealed a marked decrease in the number of viral plaques. The control group presented with 120 plaques, whereas the treated groups exhibited only 49 plaques (at 50 µg/mL) and 12 plaques (at 100 µg/mL), clearly underscoring the significant antiviral potential of the green-synthesized silver nanoparticles. In Table 2, a comparison is made of silver nanoparticles (AgNPs) that have been synthesized using various plant extracts. The table provides a range of data, including particle size, zone of inhibition (ZOI), minimum inhibitory concentration (MIC), and antiviral activity. An analysis of the table indicates that AgNPs synthesized with Ferula assa-foetida extract exhibit superior performance relative to other plant extracts. The particle size of these nanoparticles is less than 100 nm, which enhances their surface area and, as a result, their biological activity. In the antibacterial section, the diameters of the inhibition zones for Escherichia coli and Staphylococcus aureus are recorded at 14 mm and 16 mm, respectively, which surpass the majority of other samples. Furthermore, the low MIC values (25 µg/mL for S. aureus and 37.5 µg/mL for E. coli) suggest a strong antibacterial efficacy even at minimal concentrations. The antiviral activity data for AgNPs synthesized with Ferula assa-foetida include results from qPCR and plaque assays. An increase in nanoparticle concentration from 50 to 100 µg/mL resulted in a rise in the Ct value from 25.1 to 30.4 and a decrease in the number of viral plaques from 120 to 12, indicating a significant inhibition of viral replication. These results surpass those of AgNPs synthesized with extracts such as green tea or mixed plant extracts, demonstrating a more potent antiviral effect. According to Table 2, the green synthesis of silver nanoparticles using Ferula assa-foetida extract results in small, uniform particles with significant antibacterial and antiviral activities, making them attractive candidates for natural nanomedicine development. Beyond this plant, other extracts such as Wild barberry, Medlar, and Hawthorn have also yielded biologically active nanoparticles. These particles, sized between 30 and 80 nm, produced inhibition zones of 13–18 mm against both Gram-positive and Gram-negative bacteria, closely matching the antimicrobial effectiveness observed with Ferula assa-foetida.

Table 2. Comparative analysis of particle sizes, and antibacterial/antiviral activities of AgNPs synthesized using various plant extracts (*Not reported).

Planet	Extract type	Particle Size, nm	Results		Ref.
			Antibacterial	Antiviral	
Wild barberry Medlar Hawthorn	aqueous	~30-80	Zone of inhibition S. aureus:13-18mm Zone of inhibition E.Coli:11-13mm	-*	Koohestani, Nabilo, and Balooch, 2024
Ferula-gummosa essential (nanocomposite)	oil	~240-480	Zone of inhibition S. aureus:15.41mm Zone of inhibition E.Coli:16.4mm MIC for S. aureus: 0.39 µL/mL MBC for S. aureus: 3.12 µL/mL MIC for E.Coli: 0.195 µL/mL MBC for E.Coli: 0.781 µL/mL	-*	Valinezhad, Talebi, and Alamdari, 2023
Azadirachta indica	aqueous	~50-100	Zone of inhibition S. aureus:9 mm Zone of inhibition E.Coli:9 mm		Ahmed *et al.*, 2016
Green tea	aqueous	~50-10	-*	Viral titer from 9.8 to 2.1 log EID_{50} at 320 µg/mL; RNA reduced from 3×10^5 to 5×10^2 copies/mL; No cytopathic effects observed up to 320 µg/mL	Saadh, 2022
Lampranthus coccineus	aqueous	~10.12-7.89	-*	HAV-10: IC_{50} = 11.71 ng/mL HSV-1: IC_{50} = 36.36 µg/mL CoxB4: IC_{50} = 12.74 µg/mL MNTC (VERO cells): 46.87 µg/mL	Haggag *et al.*, 2019
Malephora lutea		~8.91-14.48		HSV-1: IC_{50} = 520.6 µg/mL No activity against HAV-10 and CoxB4 MNTC: 520.6 µg/mL	
Andrographis paniculata	aqueous	~70-95	-*	CPE inhibition = 75–100% (MNTD), 25–49% (½MNTD); Cell viability = 80.76 ± 1.5% (MNTD), 66.8 ± 2.1% (½MNTD).	Sharma *et al.*, 2019
Phyllanthus niruri		~70-120		PE inhibition = 25–49% (MNTD & ½MNTD); Cell viability = 75.35 ± 3.4% (MNTD), 55.98 ± 4.35% (½MNTD).	
Tinospora cordifolia		~50-70		No significant CPE inhibition; Cell viability = 30.56 ± 1.1% (MNTD), 26.47 ± 1.3% (½MNTD)	
Ferula assa-foetida		<100	CFU reduction >90% at 100 µg/mL; Disk diffusion zones: 16 mm (S. aureus), 14 mm (E. coli); MIC: 25 µg/mL (S. aureus), 37.5 µg/mL (E. coli)	CFU reduction >90% at 100 µg/mL; Disk diffusion zones: 16 mm (S. aureus), 14 mm (E. coli); MIC: 25 µg/mL (S. aureus), 37.5 µg/mL (E. coli)	This study

4. Conclusions

In this research, AgNPs were effectively synthesized via a green, environmentally friendly method utilizing Ferula assa-foetida leaf extract, and their structural and biological characteristics were comprehensively examined. FE-SEM imaging and EDX analysis indicated that the nanoparticles exhibited a spherical-to-ellipsoidal, cauliflower-like morphology with a consistent size distribution ranging from 40 to 140 nm and a high silver purity exceeding 67%, rendering them highly advantageous in terms of surface activity and bioreactivity. The findings from XRD, DLS, FT-IR, and TGA confirmed that the biosynthesized AgNPs exhibited a stable crystalline structure, with organic functional groups derived from the plant extract serving as capping agents. The biological activity assessments revealed significant antibacterial properties of the AgNPs against Gram-positive (S. aureus) and Gram-negative (E. coli) bacteria, with inhibition zones at 100 ppm comparable to the reference antibiotic gentamicin. Moreover, qPCR analysis and viral plaque assays confirmed that the AgNPs synthesized *using Ferula assa-foetida* extract (*FAgNPs*) significantly reduced viral loads and effectively inhibited viral replication in simulated hospital wastewater environments at concentrations of 50 and 100 µg/mL. When compared with previous studies utilizing plant extracts such as "*green tea"*, "Mespilus germanica", and "Ferula persica", these AgNPs displayed notably enhanced performance. This improvement can be attributed to their smaller particle size and higher surface-area-to-volume ratio, which increased their interaction with microbial membranes and viral particles. In summary, silver nanoparticles synthesized via *Ferula assa-foetida* extract not only exhibit potent antibacterial and antiviral effects but also outperform many previously reported green-synthesized AgNPs. Their strong efficacy, coupled with their eco-friendly and scalable synthesis method, positions them as a promising candidate for water disinfection and pathogen control, particularly in complex and contaminated environments such as hospital wastewater.

Nomenclature

CFU	Colony Forming Unit
CT	Cycle threshold
DLS	Dynamic light scattering
DTA	Differential thermal analysis
E. coli	Escherichia coli
EDS	Energy-Dispersive X-ray Spectroscopy
FAgNPs	The synthesized nanoparticles using Ferula extract
FE-SEM	Emission scanning electron microscopy
FLE	Ferula Assa-foetida

FTIR	Fourier-transform infrared spectroscopy
FWHM	Full width at half maximum
JCPDS	Joint Committee on Powder Diffraction Standards
MBC	Minimum Bactericidal Concentration
MIC	Minimum inhibitory concentration
OD	Optical density
PCR	Polymerase Chain Reaction
PDI	Polydispersity Index
qPCR	Real-Time quantitative PCR
ROS	Reactive Oxygen Species
S. aureus	Staphylococcus aureus
STA	Simultaneous thermal analysis
TGA	Thermogravimetric analysis
XRD	X-ray diffraction

Author Contributions

Hassan Koohestani: Methodology, Supervision, review & editing.
Ali Balooch: Methodology, Data curation, Writing - original draft.

Data Availability Statement

The datasets related to the present work are accessible from the corresponding author on request.

Conflict of Interest

The authors declare no competing interests and non-financial competing interests.

Acknowledgment

The authors are grateful for the data support provided by the laboratories at Semnan University, Semnan, Iran.

Reference

Abootalebi, S.N. *et al.* (2021) 'Antibacterial effects of green-synthesized silver nanoparticles using Ferula asafoetida against Acinetobacter baumannii Isolated from the hospital environment and assessment of their cytotoxicity on the human cell lines', *Journal of Nanomaterials*, 2021, pp. 1-12. doi: https://doi.org/10.1155/2021/6676555

Adebayo-Tayo, B., Salaam, A. and Ajibade, A. (2019) 'Green synthesis of silver nanoparticle using Oscillatoria sp. extract, its antibacterial, antibiofilm potential and cytotoxicity activity', *Heliyon*, 5(10), pp. 1-8. doi: https://doi.org/10.1016/j.heliyon.2019.e02502

Ahmed, S. *et al.* (2016) 'Green synthesis of silver nanoparticles using Azadirachta indica aqueous leaf extract', *Journal of Radiation Research and Applied Sciences*, 9(1), pp. 1–7. doi: https://doi.org/10.1016/J.JRRAS.2015.06.006

Anyanwu, E.D. *et al.* (2024) 'Spatio-temporal variations and pollution status of heavy metals in Ahi River, Ohiya, Umuahia, Nigeria', *Journal of Applied Research in Water and Wastewater*, 11, pp. 1-7. doi: https://doi.org/10.22126/arww.2024.10382.1324

Augustine, R. *et al.* (2020) 'Cellular uptake and retention of nanoparticles: Insights on particle properties and interaction with cellular components', *Materials Today Communications*, 25, pp. 1-19. doi: https://doi.org/10.1016/j.mtcomm.2020.101692

Balooch, A. *et al.* (2025) 'Experimental and computational investigation on corrosion behavior of carbon steel in the presence of Ferula assa-foetida leaf extract', *Materials Today Communications*, 42, pp. 1-8. doi: https://doi.org/10.1016/J.MTCOMM.2024.111350

Esmaile, F., Koohestani, H. and Abdollah-Pour, H. (2020) 'Characterization and antibacterial activity of silver nanoparticles green synthesized using Ziziphora clinopodioides extract', *Environmental Nanotechnology, Monitoring & Management*, 14, pp. 1-7. doi: https://doi.org/10.1016/j.enmm.2020.100303

Haggag, E.G. *et al.* (2019) 'Antiviral potential of green synthesized silver nanoparticles of lampranthus coccineus and malephora lutea', *International Journal of Nanomedicine*, 14, pp. 6217–6229. doi: https://doi.org/10.2147/IJN.S214171

Hajipour, M.J. *et al.* (2012) 'Antibacterial properties of nanoparticles', *Trends in Biotechnology*, 30, pp. 499-511. doi: https://doi.org/10.1016/j.tibtech.2012.06.004

Hashemi, Z. *et al.* (2022) 'Sustainable biosynthesis of metallic silver nanoparticles using barberry phenolic extract: Optimization and evaluation of photocatalytic, in vitro cytotoxicity, and antibacterial activities against multidrug-resistant bacteria', *Inorganic Chemistry Communications*, 139, pp. 1-12. doi: https://doi.org/10.1016/j.inoche.2022.109320

John, A. *et al.* (2021) 'Anti-bacterial and biocompatibility properties of green synthesized silver nanoparticles using Parkia biglandulosa (Fabales:Fabaceae) leaf extract', *Current Research in Green and Sustainable Chemistry*, 4, pp. 1-7. doi: https://doi.org/10.1016/j.crgsc.2021.100112

Joshi, A.S., Singh, P. and Mijakovic, I. (2020) 'Interactions of gold and silver nanoparticles with bacterial biofilms: Molecular interactions behind inhibition and resistance', *International Journal of Molecular Sciences*, 21, pp. 1–24. doi: https://doi.org/10.3390/ijms21207658

Kędziora, A. *et al.* (2018) 'Similarities and differences between silver ions and silver in nanoforms as antibacterial agents', *International Journal of Molecular Sciences*, 19, pp. 1-17. doi: https://doi.org/10.3390/ijms19020444

Koohestani, H., Balooch, A. and Hasanpoor, J. (2024) 'Utilizing gum Commiphora Mukul as organic binders to replace bentonite in iron Ore Pelletizing ARTICLE INFO', *International Journal of ISSI*, 21, pp. 39-46. doi: https://doi.org/10.22034/IJISSI.2025.2044698.1308

Koohestani, H. and Gohariyan Bajestani, A. (2025) 'Use of semi-coke as Pb ion adsorbent from polluted industrial wastewater', *Journal of Applied Research in Water and Wastewater*, 12, pp. 51-85. doi: https://doi.org/10.22126/arww.2025.11292.1347

Koohestani, H., Nabilo, M. and Balooch, A. (2024) 'Biosynthesis and investigation of antibacterial properties of green silver nanoparticles using fruit extracts of Wild barberry, Medlar (Mespilus germanica L.), and Hawthorn', *Food Chemistry Advances*, 6, pp. 1-7. doi: https://doi.org/10.1016/j.focha.2024.100850

Labulo, A.H., David, O.A. and Terna, A.D. (2022) 'Green synthesis and characterization of silver nanoparticles using Morinda lucida leaf extract and evaluation of its antioxidant and antimicrobial activity', *Chemical Papers*, 76, pp. 7313-7325. doi: https://doi.org/10.1007/s11696-022-02392-w

Mikhailova, E.O. (2020) 'Silver nanoparticles: mechanism of action and probable bio-application', *Journal of Functional Biomaterials*, 11, pp. 1-26. doi: https://doi.org/10.3390/jfb11040084

Mohammadhosseini, M. *et al.* (2019) 'The genus Ferula: Ethnobotany, phytochemistry and bioactivities - A review', *Industrial Crops and Products*, 129, pp. 350-394. doi: https://doi.org/10.1016/j.indcrop.2018.12.012

Naeini, A.H. (2025) 'Investigating the adsorption method using polymer nanocomposites as adsorbent to remove organic pollutants: A review', *Journal of Applied Research in Water and Wastewater*, 12, pp. 19-51. doi: https://doi.org/10.22126/arww.2025.9872.1315

Nasiri, J. *et al.* (2018) 'Fulfillment of green chemistry for synthesis of silver nanoparticles using root and leaf extracts of Ferula persica: Solid-state route vs. solution-phase method', *Journal of Cleaner Production*, 192, pp. 514-530. doi: https://doi.org/10.1016/j.jclepro.2018.04.218

Nie, P., Zhao, Y. and Xu, H. (2023) 'Synthesis, applications, toxicity and toxicity mechanisms of silver nanoparticles: A review', *Ecotoxicology and Environmental Safety*, 253, pp. 1-12. doi: https://doi.org/10.1016/j.ecoenv.2023.114636

Rasheed, A. *et al.* (2023) 'Application of silver nanoparticles synthesized through varying biogenic and chemical methods for wastewater treatment and health aspects', *Environmental Science and Pollution Research*, 30, pp. 1-19. doi: https://doi.org/10.1007/s11356-022-24761-4

Roy, A. *et al.* (2019) 'Green synthesis of silver nanoparticles: Biomolecule-nanoparticle organizations targeting antimicrobial activity', *RSC Advances*, 9, pp. 2673-2702. doi: https://doi.org/10.1039/c8ra08982e

Saadh, M. (2022) 'Potent antiviral effect of green synthesis silver nanoparticles on Newcastle disease virus', *Arabian Journal of Chemistry*, 15, pp. 1-5. doi: https://doi.org/10.1016/j.arabjc.2022.103899

Sahebkar, A. and Iranshahi, M. (2010) 'Biological activities of essential oils from the genus Ferula (Apiaceae)', *Asian Biomedicine*, 11, pp. 1-28. doi: https://doi.org/10.2478/abm-2010-0110

Salehi Reyhani, Z. and Khoshnood, Z. (2020) 'Study of biofilm creating bacteria in drinking water of Ahvaz city in Iran', *Journal of Applied Research in Water and Wastewater*, 7, pp. 163-166. doi: https://doi.org/10.22126/arww.2020.4435.1140

Seki, Y. *et al*. (2013) 'Extraction and properties of Ferula communis (chakshir) fibers as novel reinforcement for composites materials', *Composites Part B: Engineering*, 44(1), pp. 517-523. doi: https://doi.org/10.1016/j.compositesb.2012.03.013

Sharma, V. *et al*. (2019) 'Green synthesis of silver nanoparticles from medicinal plants and evaluation of their antiviral potential against chikungunya virus', *Applied Microbiology and Biotechnology*, 103, pp. 881-891. doi: https://doi.org/10.1007/s00253-018-9488-1

Slavin, Y.N. *et al*. (2017) 'Metal nanoparticles: Understanding the mechanisms behind antibacterial activity', *Journal of Nanobiotechnology*, 15, pp. 1-20. doi: https://doi.org/10.1186/s12951-017-0308-z

Smuleac, V. *et al*. (2011) 'Green synthesis of Fe and Fe/Pd bimetallic nanoparticles in membranes for reductive degradation of chlorinated organics', *Journal of Membrane Science*, 379 (1-2), pp. 131-137. doi: https://doi.org/10.1016/j.memsci.2011.05.054

Subramaniam, S. *et al*. (2022) 'Spectral and structure characterization of Ferula assafoetida fabricated silver nanoparticles and evaluation of its cytotoxic, and photocatalytic competence', *Environmental Research*, 204, pp. 1-11. doi: https://doi.org/10.1016/j.envres.2021.111987

Taleb Safa, M.A. and Koohestani, H. (2024) 'Green synthesis of silver nanoparticles with green tea extract from silver recycling of radiographic films', *Results in Engineering*, 21, pp. 1-6. doi: https://doi.org/10.1016/j.rineng.2024.101808

Valinezhad, N., Talebi, A.F. and Alamdari, S. (2023) 'Biosynthesize, physicochemical characterization and biological investigations of chitosan-Ferula gummosa essential oil (CS-FEO) nanocomposite', *International Journal of Biological Macromolecules*, 241, pp.1-11. doi: https://doi.org/10.1016/j.ijbiomac.2023.124503

Zadeh, S.H., Kashanian, S. and Nazari, M. (2024) 'Identification of pathogenic bacteria by biosensors in water and wastewater', *Journal of Applied Research in Water and Wastewater*, 11, pp. 169-175. doi: https://doi.org/10.22126/arww.2024.9677.13